DEUTSCHES ELEKTRONEN-SYNCHROTRON DESY

DESY SR-75/03
April 1975

Excitons and Continuum Transitions of Rubidium Halides in the 10 - 26 eV Photon Energy Range at Low Temperatures

by

W. Zierau and M. Skibowski
Sektion Physik der Universität München

2 HAMBURG 52 · NOTKESTIEG 1

To be sure that your preprints are promptly included in the
HIGH ENERGY PHYSICS INDEX ,
send them to the following address (if possible by air mail) :

DESY
Bibliothek
2 Hamburg 52
Notkestieg 1
Germany

EXCITONS AND CONTINUUM TRANSITIONS OF RUBIDIUM HALIDES IN THE 10 - 26 eV PHOTON ENERGY RANGE AT LOW TEMPERATURES.†

Wolfgang Zierau* and Michael Skibowski**,
Sektion Physik der Universität München,
München, Germany

† Work supported by the Deutsches Elektronen-Synchrotron, DESY, Hamburg, Germany

* Now at Institut für theoretische Physik II, Universität Münster, Münster, Germany, on leave of absence University of California, Irvine, California 92664, USA

** Now on leave of absence at Xerox Palo Alto Research Center, Palo Alto, California and University of Illinois, Urbana, USA

accepted for J. Phys. C

Abstract

The reflection spectra of RbCl, RbBr and RbI single crystals were investigated for temperatures between 300 K and 8 K in order to study excitations from the Rb^+4p level ($\gtrsim$ 16 eV) as well as the higher continuum transitions from the valence band ($\gtrsim$ lo eV). The measurements were performed by use of the synchrotron radiation of DESY. The sensitivity for detecting details of the fine structure was increased by simultaneously measuring the wavelength modulated spectra. The experimental procedure is briefly described. New spectral features have been resolved for the exciton multiplets from the Rb^+4p level. They are discussed in light of the predictions of a recent model for the Rb^+4p excitons based on ligand field theory. The continuum transitions associated with the valence band and the Rb^+4p level show characteristic structure which is compared with calculations of the joint density of states.

1. Introduction

During the past considerable interest has been devoted to the investigation of the excitons from the valence band in alkali halides (e.g. Baldini and Bosacchi 1968 and 1970). The valence band is formed by the outermost p electrons of the halide ion. For most alkali halides photon energies below 10eV are sufficient to excite these electrons into prominent excitonic states, a result of strong electron-hole interaction in these materials. For excitation of the outer shell electrons of the alkali ion higher energies above 13eV are necessary. At the onset of the alkali transitions the excitation spectra also show multiplets of sharp lines. These were interpreted as excitons associated with the core level of the alkali ion, analogous to the observations in the valence band regime. In particular the Rb-halides show very prominent multiplets between 16 and 18 eV first observed by Peimann and Skibowski (1971) and Saile, Schwentner, Skibowski, Steinmann and Zierau (1973) in reflection and by Watanabe et al. (1971) in absorption. The variety of the multiplets could not be explained satisfactorily in terms of the band structure as is usually done for the charge transfer type excitons associated with the valence band. Instead this multiplet has been interpreted as being localized excitations from the Rb^+4p level by comparison with the five low-lying dipole allowed excitations of the free Rb^+ion.

Starting from this simple free ion model a more sophisticated localized model on the basis of the ligand field theory (e.g. Sugano, Tanabe and Kamimura 1970) has recently been proposed by Satoko and Sugano (1973). This model takes into account the influence of the octahedral field produced by the surrounding nearest halogen neighbours and seemed to be capable of describing the previously observed quintet structure. In addition the occurrence of four low-energy excitons from the Rb^+4p level originating from $\tilde{p}d\epsilon$ configuration has been predicted.

One aim of our work was to test the predictions of the ligand field model. In order to obtain high experimental resolution the optical spectra were investigated at temperatures down to 8K including wavelength modulation. Secondly we wanted to study in more detail the spectra in the neighbouring continua associated with excitations of both, the halide valence electrons (<16eV) and the Rb^+4p electrons (>19eV). Recent calculations of the joint density of states (Overhof 1973) enabled us to make comparisons with the spectra of the imaginary part of the dielectric constant, ϵ_2, calculated from our reflection measurements.

2. Experimental

2.1 General

Using the continuum of the synchrotron radiation of the DESY electron synchrotron together with a normal incidence monochromator (Koch and Skibowski 1971) the reflection spectra of Rb-halide single crystals were measured between room temperature

and 8K. The spectral resolution was 2 Å i.e. about 40 meV at 16 eV. The whole experimental set-up is shown schematically in figure 1. The single crystals were freshly cleaved in air and then immediately transferred into a reflectometer in an ultrahigh-vacuum-sample-chamber. The pressure during the measurements was about $3\text{-}4 \cdot 10^{-10}$ Torr. The single crystals were cooled by a liquid Helium cryostat.

Primarily we were interested in measuring the positions of the spectral structures and their relative heights in the reflection spectra, which were obtained by use of an open magnetic multiplier. We performed a Kramers-Kronig analysis to derive the imaginary part of the dielectric constant, ε_2, and the absorption coefficient, μ, from our measured spectra. For this we needed the absolute reflectivity values. There is some uncertainty in these because of well known difficulties in positioning and the response inhomogeneity of the multiplier used. At room temperature the absolute reflectivity of the highest peaks in the 16 - 19 eV range was approximately 10%.

2.2 Wavelength modulation with synchrotron radiation

Besides simple reflection spectra wavelength modulated reflectivities (for general reviews Cardona 1969 and Batz 1972) were additionally measured aiming at higher sensitivity for fine structure. Synchrotron radiation as a continuous light source, although pulsed, provided an excellent light source in the vacuum-ultraviolet (VUV) for wavelength modulation (Zierau 1973

and 1974). Up till now wavelength modulation was limited to dc light sources in the UV and the near VUV below 6eV. The common methods of modulating the wavelength by vibrating mirrors or plates (Batz 1972) are difficult to use in the vacuum-ultraviolet as there is a serious loss of intensity by any reflection or transmission. As an alternative, we have chosen periodical vibration of the grating of our normal incidence monochromator (figure 1). Wavelength scanning is achieved by rotating the grating around an eccentric axis by a wire connected to a linear feedthrough.

An electrodynamical system vibrating at the frequency $\omega_1 = 2\pi\nu_1$ periodically pushes the elastic wire and causes small oscillations of the angle of dispersion around a center wavelength λ_o so that the wavelength is modulated in first order by:

$$\lambda(t) = \lambda_o + \Delta\lambda \sin(\omega_1 t + \varphi) \qquad (1)$$

$\Delta\lambda$ and φ being the amplitude and phase resp. The phase φ is measured with respect to the light incident on the sample which can be represented in lowest order by:

$$I_o(\lambda\ ,\ t) = \bar{I}_o(\lambda)\ (1 + a \sin\omega_o t) + \ldots \qquad (2)$$

where $\omega_o = 2\pi\nu_o$ is the operational frequency of the synchrotron (50 cps) and a is considered to be a constant in our wavelength range.

The measured intensity reflected from the sample is:

$$I_R(\lambda(t)\ ,\ t) = R(\lambda(t))\ I_o(\lambda(t)\ ,\ t) \qquad (3)$$

where $R(\lambda)$ is the reflectivity of the sample. The normalized derivative of the reflectivity

$$\frac{1}{R}\frac{dR}{d\lambda}\Big|_{\lambda_o} \equiv \frac{\Delta R}{R} \cdot \frac{1}{\Delta\lambda}$$

is to be determined experimentally. We obtain the desired quantity from expansion of $I_R(\lambda(t)\ ,t\ )$ for small modulation amplitudes $\Delta\lambda$ for any time t:

$$I_R(\lambda(t)\ ,\ t\ ) = I_R(\lambda_o\ ,\ t\ ) + \frac{dI_R(\lambda,\ t\ )}{d\lambda}\Big|_{\lambda_o} \Delta\lambda\ \sin(\omega_1 t + \varphi) + \ldots \qquad (4)$$

Inserting equation (2) and (3) into (4) one obtains an expression containing, as far as the time dependence is concerned, only terms with frequencies ω_o, ω_1 and $\omega_o + \omega_1$, $\omega_o - \omega_1$. In the case $\varphi = 0$ and assuming $\omega_1 = \omega_o/2$(i.e.ν_1 = 25cps) it is considerably simplified and reduces to:

$$I_R(\lambda(t),t) = R(\lambda_o)\cdot\bar{I}_o(\lambda_o) + R(\lambda_o)\cdot\bar{I}_o(\lambda_o)\cdot 2\tan\alpha\cdot\sin\omega_o t \qquad (5)$$

$$+ \left.\frac{d(R(\lambda)\bar{I}_o(\lambda))}{d\lambda}\right|_{\lambda_o} \cdot\Delta\lambda\cdot \left\{(\cos\alpha)^{-1}\sin(\omega_1 t+\alpha)\right.$$

$$\left. + \tan\alpha\cdot\cos 3\omega_1 t\right\} + \ldots$$

where α is defined by $\tan\alpha = \frac{a}{2}$ and the constant a is determined by the incident synchrotron radiation (cf. equation(2)). An equivalent equation can be derived in case of $\varphi = \frac{\pi}{2}$.

By phase-sensitive detection, tuning Lock-In-Amplifier 2 (figure 1) at $\omega_o(\nu_o = 50\text{cps})$ and Lock-In-Amplifier 3 at $\omega_1(\nu_1 = 25\text{cps})$ and appropriate phase adjustment, one measures the amplitudes

$$I_R \equiv R(\lambda_o)I(\lambda_o)2\tan\alpha \text{ and } \Delta I_R \equiv \left.\frac{d(R(\lambda)\bar{I}_o(\lambda))}{d\lambda}\right|_{\lambda_o} \Delta\lambda(\cos\alpha)^{-1} .$$

Electronic division of both amplitudes yields

$$\frac{\Delta I_R}{I_R} = (2\sin\alpha)^{-1} \left\{ \frac{1}{\bar{I}_o(\lambda_o)} \left.\frac{d\bar{I}_o(\lambda)}{d\lambda}\right|_{\lambda_o} \Delta\lambda + \frac{1}{R(\lambda_o)} \left.\frac{dR(\lambda)}{d\lambda}\right|_{\lambda_o} \Delta\lambda \right\} \quad (6)$$

where the differentiation of the product $R(\lambda)\bar{I}_o(\lambda)$, has been carried out. The first term of equation (6), which represents the contribution of the spectral distribution of the incident light, was measured separately without sample. It contains no significant structure. Therefore by simply subtracting numerically, one obtains the desired quantity

$$\frac{1}{R(\lambda_o)} \left.\frac{dR(\lambda)}{d\lambda}\right|_{\lambda_o} \Delta\lambda = \frac{1}{R(E_o)} \cdot \frac{dR(E)}{dE} \left.\frac{dE}{d\lambda}\right|_{E_o} \Delta\lambda \quad (7)$$

The normalized derivative with respect to the photon energy E is reported in our results (chapter 3).

Our spectra were usually measured with a modulation amplitude of $\Delta\lambda = 2\text{Å}$. We obtained a sensitivity for the detection of structure of $5\cdot10^{-2}\text{eV}^{-1}$. Slow fluctuations of the

intensity of the synchrotron radiation as well as detector instabilities were compensated by the described method since the same detector is used in the measurement of I_R and ΔI_R .

In addition to $\Delta I_R/I_R$ we determined $I_R/\langle I \rangle$ (figure 1). $\langle I \rangle$ is the photocurrent of a Cu-Be-plate which is detected by Lock-In-Amplifier 1. It represents a measure of the total light flux incident on the grating. $\bar{I}_o/\langle I \rangle$ was measured without the sample. The relative reflectivity $R = I_R/\bar{I}_o$ is then obtained by numerical division.

3. Experimental Results

A comparison of the spectra of RbCl, RbBr and RbI is shown for room temperature and at 8K in figure 2. For each crystal the reflection spectrum and its simultaneously recorded normalized derivative are plotted together. The pronounced multiplets observed for all the halides in the 16 - 19 eV photon energy range which are associated with the excitons from the Rb^+4p level closely resemble each other even at low temperatures.

Below 16eV the region, where valence band transitions occur, no significant similarity in the spectral features can be observed. Structure is pronounced at 8K and further structure emerges in the wavelength modulated

spectra. A characteristic triplet is resolved for RbBr around 15 eV . As compared to RbCl and RbBr, RbI shows a much greater variety of structure in the low energy region which sharpens considerably at low temperatures.

Above 19 eV, the region likely to be dominated by continuum transitions from the Rb^+4p level, the spectra look similar in that a correspondence between the broad maxima F, G and H can be established. The structure F in RbI, however, can only be seen as a shoulder in the modulated spectra at low temperatures.

The excitonic region is represented in detail in figure 3. New remarkable spectral features occur at low temperatures: RbCl and RbBr show a distinct peak X at 8K with an additional weak shoulder X', clearly resolved in the modulated spectra. For RbI corresponding structure X and X' together with the unresolved peak C are detected in the modulated spectra. A further shoulder Y shows up in the spectra of RbBr and is also detected as a characteristic change of slope in the wavelength modulated spectra of RbCl and RbI. In RbI, when the temperature is decreased from liquid nitrogen temperature (LNT) to 8K, the relative heights of the first excitons A and B are inverted. Simultaneously the strengths of the valence band transitions (figure 2) increase and the peak below A (15.8 eV) splits into U and V. This splitting is already indicated at room temperature in the modulated spectra.

The optical constants ε_2 and μ have been calculated by a Kramers-Kronig analysis from our reflection data. In comparison to the reflection spectra no extraordinary changes in the relative heights and the positions of the peaks were found in the μ and ε_2 spectra.

The energy positions of the different spectral features can be determined very accurately from the modulated and the unmodulated spectra together. In table 1 and table 2 the positions are listed for 300 K and 8K. The calculated values of the ε_2 - spectra are listed, as well.

Absorption measurements on evaporated thin films at liquid nitrogen temperature have been performed by Watanabe et al. (1971). Figure 4 shows a comparison with our calculated μ-spectrum at 8K. The main structure agrees quite well. But several new features observed in our spectra cannot be seen in the absorption spectra of Watanabe et al. (1971).

4. Discussion

4.1. Rb^+4p - Excitons

The close similarity of the multiplets in the 16 - 19 eV photon energy range for the different Rb-halides (figure 3) provides strong support for the assumption that these peaks are due to localized excitons of the Rb^+4p level. Apparent differences are attributed to the influence of the surrounding ions.

The temperature dependence of the observed sturctures and their shift as a function of the different halide ion enables us to correlate peaks in the different spectra (figure 5). With the exception of the A-exciton of RbI all structure shifts to higher energies with the lighter ionmass. Furthermore, the temperature dependence differs for the different excitonic lines. Whereas the A and C exciton shifts to higher energies at low temperatures, the B, C, D and E excitons shift to lower energies. Less can be said about the new structure X', X and Y. They are rapidly vanishing at elevated temperatures even in the modulated spectra (> 120K).

The first step in the interpretation of the data (Peimann and Skibowski 1971) is to compare the positions of the main features with those of the five low-lying dipole allowed transitions (J=1) of the free Rb^+ ion (Moore 1958), represented by the bars at the bottom of figure 5. Three low-lying J=2 transitions are additionally marked.

The correspondence to the observed excitonic peaks A,B,C, D,E can tentatively be established as follows:

A: $4p^6 \rightarrow 5s[3/2]$ 16.72 eV

C: $4p^6 \rightarrow 5s'[1/2]$ 17.78 eV

B: $4p^6 \rightarrow 4d[1/2]$ 15.68 eV

D: $4p^6 \rightarrow 4d[3/2]$ 17.43 eV

E: $4p^6 \rightarrow 4d'[3/2]$ 18.05 eV

Closer inspection shows that the simple ionic model only provides a rough description of the observed spectra.

It can be refined by additionally taking into account the effect of the electric field of the surrounding halide ions (ligand field) (Satoko and Sugano 1973).

One assumes that the "hole", which is left by excitation of the electron, is localized at the Rb^+ ion, the point symmetry of the ligand field being O_h. The terms arise from configurations $t_{1u}^5 a_{1g}$, $t_{1u}^5 t_{2g}$ and $t_{1u}^5 e_g$ ($p^5 s$, $p^5 d\varepsilon$, $p^5 d\gamma$ resp. $p^5 \equiv \tilde{p}$ in figure 6), to which optical transitions from the ground state $t_{1u}^6 A_{1g}$ are allowed. t_{1u}, a_{1g}, t_{2g} and e_g are the symmetry adapted linear combinations of the 4p, 5s, 4dε and 4dγ one-electron orbitals of the Rb^+ ion. The term energies are calculated assuming reasonable wave functions including Coulomb interaction, spin-orbit interaction and cubic field splitting. The term energies are obtained as a function of the crystal field parameter Dq. The relative oscillator strengths are calculated as well. Figure 6 shows the term energies of the ligand field model (left side) and the oscillator strengths for RbBr as an example (right side) together with the ε_2-spectrum calculated from the measured reflection spectrum at 8K. Nine low-lying terms are predicted by the model. Only five A, B, C, D, E have been observed in previous work (Peimann and Skibowski 1971, Watanabe et al. 1971). In figure 3 the calculated term energies and their relative oscillator strengths are represented by the bars at the bottom.

Comparison to the measured spectra shows that there is no relevant structure attributable to the predicted $d\varepsilon$-transitions (I, II, III and IV). Even the wavelength modulated spectra at 8K do not contain a hint of their existence. The triplet around 15 eV observed in the case of RbBr (figure 6) is assumed to be due to transitions from the valence band. Such triplet structure is presumably associated with the Br^- ion in alkali halides (Baldini and Bosacchi 1968 and 1970). There is no equivalent structure in the spectra of the other Rb-halides. It is not quite clear why the predicted transitions cannot be seen in the experimental spectra. Possibly they are still hidden under the valence band transitions because they are too weak.

On the other hand all our spectra show new structures X', X and Y which obviously belong to excitations of the Rb^+4p level (figure 5). They are not predicted by the ligand field model. The new structure X' and Y, separated by about 0.8 - 0.9 eV, may correspond to the onset of the continuum transitions from the spin-orbit split Rb^+4p level. The spin-orbit splitting of the free Rb^+ ion is about 0.9 eV (Moore 1958). Results from photoemission locate the onset at about 16.8 eV for RbI (Blechschmidt et al. 1971) and 17.2 eV for RbCl (Veseley and Langer 1972). The additionally observed peak X can be understood in terms of the ligand field model by assigning X to an excited state of the exciton with a more extended molecular cluster (Sugano 1974).

Besides the temperature dependent inversion of the intensities of A and B excitons in RbI starting below LNT is not derived in the ligand field model. It may be caused by a temperature dependent configuration interaction of the Rb^+4p excitons with the strong valence band transitions.

4.2. Continuum transitions

In addition to the exciton transitions discussed above, the low temperature measurements exhibit considerable structure in the region of the continuum transitions from the valence band (<16 eV) and from the Rb^+4p level (>19 eV) at low temperatures (figure 2). RbI shows especially strong temperature dependent effects in the valence band region below 15.6 eV, obviously associated with the I^- ion. A similar behaviour was already observed for other alkali iodides (Blechschmidt et al.1971, Saile and Skibowski 1972).

A possible method for the interpretation of the continuum spectra is to assume direct interband transitions. In this case structure in the region of continuum transitions should resemble to the joint density of states, if transition matrix elements are considered to be constant. Calculations of the energy band structure of the Rb-halides have been performed by Kunz (1970) with a nonrelativistic OPW method. Overhof (1973) calculated the energy bands using the relativistic Greens function method (figure 7). From his bands he evaluated the joint density of states curves for the different Rb-halides.

A comparison with the ε_2 - spectra calculated from our reflection measurements is presented in figure 8. As expected joint density of states calculations do not give maxima as sharp as those related to the Rb^+4p excitons. A fair and by no means unambiguous correspondence in the gross structure can be established between experiment and calculation. It seems as if the pronounced finer structure detected in the measured spectra at 8K is also reproduced in Overhof's calculations.

Above 19 eV the spectra of the different Rb-halides look similar with broad maxima associated with additional structure superimposed. The main peaks G and H shift to higher energies for the compounds with the lighter ion. The shift has the same direction which we have already observed for the Rb^+4p excitons (figure 5). This is attributable to the differences in the crystal field influencing the Rb^+4p level.

All in all, the agreement between the joint density of states and measured ε_2-spectra is not satisfactory in all respects. Possibly major differences may be explained by non-negligible electron-hole interaction which presumably modifies considerably the continuum transitions.

Acknowledgements

We are grateful to Professor W. Steinmann for initiating

wavelength modulation with synchrotron radiation and for many valuable discussions during the course of this work. We would like to thank Dipl. Phys. V. Saile and Dipl. Phys. N. Schwentner for help in the first stages of the experiment and Professor S. Sugano and Dr. H. Overhof for valuable discussions. We are grateful to the staff of the synchrotron radiation group at DESY for technical support. W. Z. acknowledges the financial support of the Studienstiftung des deutschen Volkes.

References

Batz B. 1972 "Semiconductors and Semimetals" vol. 9 ed. R.K. Willardson and A. C. Beer (New York:Academic Press) pp 315 - 402

Baldini G. and Bosacchi B. 1968 Phys. Rev. 166, 863-70

Baldini G. and Bosacchi B. 1970 Proc. X Europ. Congr. Molecular Spectroscopy Liege 1969 (Liege: University Press) pp 305 - 24

Blechschmidt D., Haensel R., Koch E.E., Nielsen U. and Skibowski M. 1971 phys. stat. sol. (b) 44, 787-93

Blechschmidt D., Saile V., Skibowski M. and Steinmann W. 1971 unpublished

Cardona M. 1969 "Modulation Spectroscopy" Sol.Stat. Phys. suppl. 11 (New York: Academic Press)

Koch E.E. and Skibowski M. 1971 Chem. Phys. Lett. 9, 429 - 432

Kunz A.B. 1970 J. Phys. Chem. Sol. 31, 265 - 74

Moore C.E. 1958 "Atomic Energy Levels", NBS-Circular, No. 467 Vol. 2

Overhof H. 1973 unpublished

Peimann C. J. and Skibowski M. 1971 phys. stat. sol. (b)46, 655-65

References (continued)

Saile V. and Skibowski M. 1972 phys. stat. sol. (b) 50, 661 - 72

Saile V., Schwentner N., Skibowski M., Steinmann W. and Zierau W. 1973 Phys. Lett. 46 A, 245 - 6

Satoko C. and Sugano S. 1973 J. Phys. Soc. Japan 34, 701 - 10

Sugano S., Tanabe Y. and Kamimura H. 1970 "Multiplets of Transition-Metal Ions in Crystals" (New York: Academic Press)

Sugano S. 1974 private communication

Veseley C. J. and Langer D. W. 1972 unpublished

Watanabe M., Ejiri A., Yamashita H., Saito H., Sato S., Shigabuchi T. and Nishida H. 1971 J. Phys. Soc. Japan 31, 1085 - 91

Zierau W. 1973 Proc. Int. Symp. Synchrotron radiation users, Daresbury, ed G.V. Marr and I.H. Munro (Science Research Council, DNPL) DNPL/R26 pp 317 - 20

Zierau W. 1974 Thesis, Universität München

Table 1: Structures in the transitions from the valenceband

a) RbCl

	R		ε_2
	8 K	300 K	8 K
peak (strong)	12.24	12.06	11.94
shoulder	12.75		12.75
peak (weak)	13.03		13.02
shoulder		13.52	
peak (weak)	13.70		13.65
shoulder	14.70		14.80
shoulder	15.60		
shoulder	15.90		

b) RbBr

	R		ε_2
	8 K	300 K	8 K
peak (weak)	10.95		10.80
shoulder		10.86	
peak (strong)	11.30	11.28	11.10
peak	11.53		11.44
shoulder		11.80	
shoulder	11.90		11.76
shoulder	12.18		12.05
shoulder	12.65		
peak	14.95		14.92

b) RbBr

	R		ε_2
	8 K	300 K	8 K
peak	15.20	15.42	15.18
peak	15.51		15.50

c) RbJ

	R		ε_2
	8 K	300 K	8 K
peak	10.74	10.56	10.63
peak	10.98		10.90
shoulder		10.98	
peak	11.26		11.15
shoulder		11.26	
peak	11.77		11.71
peak	12.98	12.80	12.91
peak	13.25		13.22
peak	14.02	13.88	13.98
peak	14.93	14.59	14.85
peak U	15.78	15.52	15.72
peak V /	15.96		
shoulder V		15.72	15.91

Table 2: Structures in the transitions from the Rb^+4p level

a) RbCl

	R		ε_2	
	8 K	300 K	8 K	300 K
exciton A	16.22	16.10	16.20	16.07
exciton B	16.64	16.66	16.64	16.69
shoulder X'	16.83			
peak X	17.00		16.99	
exciton C	17.12	16.98	17.09	16.96
exciton D	17.43	17.46	17.37	17.38
shoulder Y	17.80			
exciton E	18.10	18.17	18.06	18.07
peak F	18.87	18.60	18.71	
peak G	21.89	21.85	21.61	21.25
peak H	24.70	24.68	24.40	24.15

b) RbBr

	R		ε_2	
	8 K	300 K	8 K	300 K
exciton A	16.14	16.09	16.12	16.03
exciton B	16.55	16.64	16.55	16.65
shoulder X'	16.77			
peak X	16.91		16.91	
exciton C	17.025	16.98	17.025	16.94
exciton D	17.31	17.39	17.26	17.31

b) RbBr

	R		ε_2	
	8 K	300 K	8 K	300 K
shoulder Y	17.56		17.55	
exciton E	18.02	18.14	17.94	18.06
peak F	18.29		18.22	
peak G	21.31	21.40	21.00	20.80
peak H	23.87	23.95	23.70	23.55

c) RbJ

	R		ε_2	
	8 K	300 K	8 K	300 K
exciton A	16.30	16.21	16.28	16.14
exciton B	16.47	16.49	16.54	16.56
shoulder X'	16.75			
shoulder X	16.89			
shoulder C	17.01	16.85		
exciton D	17.13	17.12	17.04	17.02
shoulder Y	17.55			
exciton E	17.94	17.96	17.86	17.88
shoulder F	18.3			
peak G	21.14	20.85	21.00	20.17
peak H	23.92	23.62	23.65	22.82

Figure Captions

Fig. 1 A sketch of the experimental set-up for the measurement of the reflectivity and its normalized derivative with respect to wavelength, using a single detector (For details cf chapter 2.2)

Fig. 2 Reflection spectra of the Rb-halides and their measured derivative at room temperature (dashed line) and at 8K (solid line).

Fig. 3 Reflection spectra of the Rb-halides and the measured derivative in the region of the Rb^+4p excitons at room temperature and at 8K together with the ϵ_2-spectra obtained from a Kramers-Kronig analysis. The bars at the bottom denote the positions and the relative oscillator strengths of the transitions according to the ligand field model by Satoko and Sugano (1973). (I, II, III, IV; A, C; B, D, E corresponding to $\tilde{p}d\varepsilon$, $\tilde{p}s$, $\tilde{p}d\gamma$ configuration.)

Fig. 4 Absorption coefficient μ at 8K (solid line) calculated from our reflection data and at 90K (dashed line) of Watanabe et al. (1973). The data are normalized to the highest excitonic maximum.

Fig. 5 Shift of peaks and shoulders with temperature

Figure Captions (continued)

(dashed-dotted line). The size of the symbols denotes the error (□ RbCl, △ RbBr, ○ RbI). Positions of low-lying transitions of the free Rb^+ ion in this region (Moore 1958) are represented by the bars at the bottom.

Fig. 6 Term energies as a function of the ligand field parameter Dq (left side) and the appropriate oscillator strengths of RbBr (right side) reproduced from Satoko and Sugano (1973). The experimental ϵ_2-spectrum at 8K is also shown on the right side. Structure X', X and Y is not derived by the ligand field model.

Fig. 7 Energy band structure of RbI reproduced from Overhof (1973).

Fig. 8 Comparison of the measured ϵ_2-spectra at 8K to the joint density of states calculated by Overhof (1973).

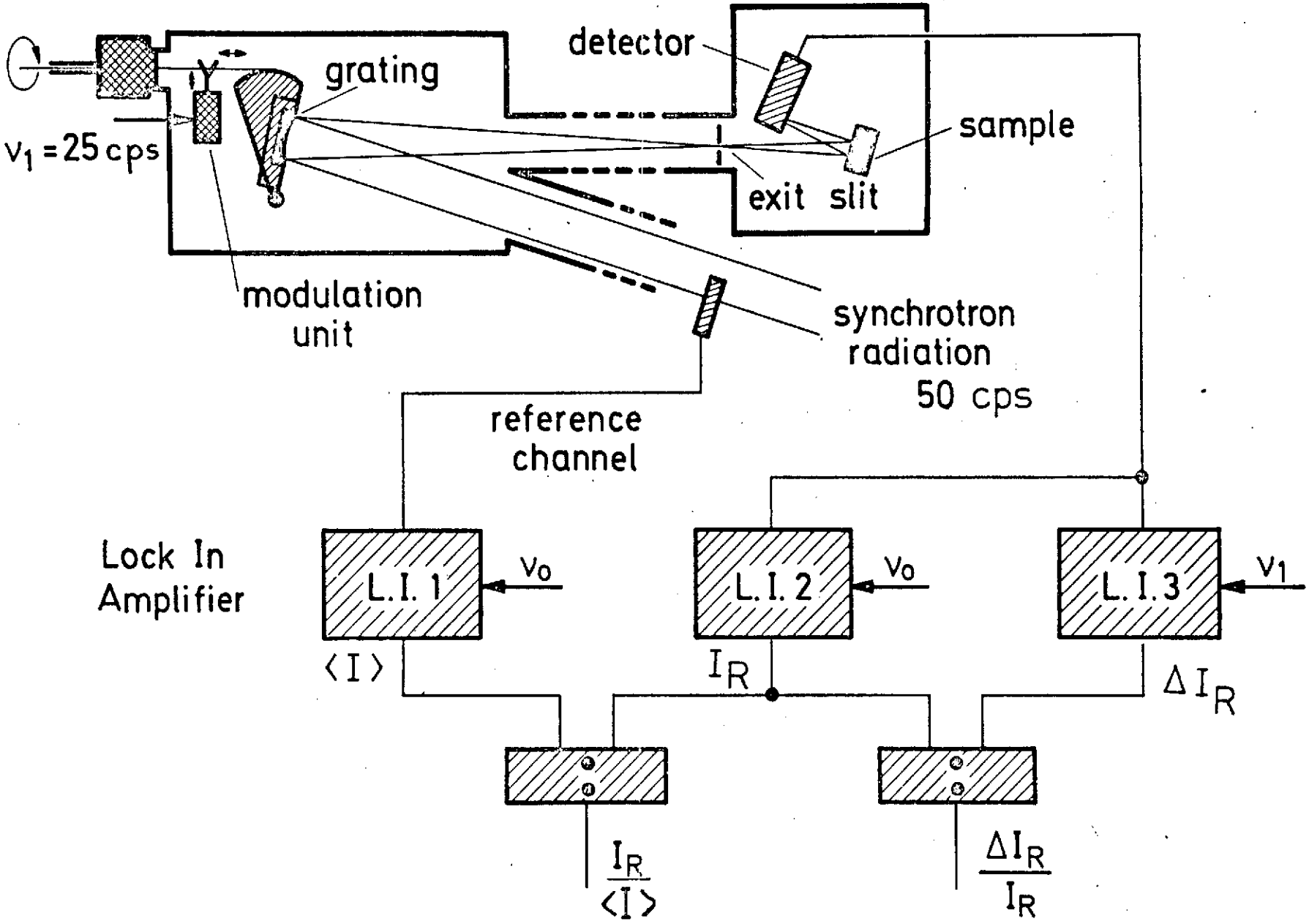
detector
grating
sample
$\nu_1 = 25$ cps
exit slit
modulation unit
synchrotron radiation 50 cps
reference channel
Lock In Amplifier
L.I. 1
L.I. 2
L.I. 3
ν_0
ν_0
ν_1
$\langle I \rangle$
I_R
ΔI_R
$\frac{I_R}{\langle I \rangle}$
$\frac{\Delta I_R}{I_R}$

Fig. 1

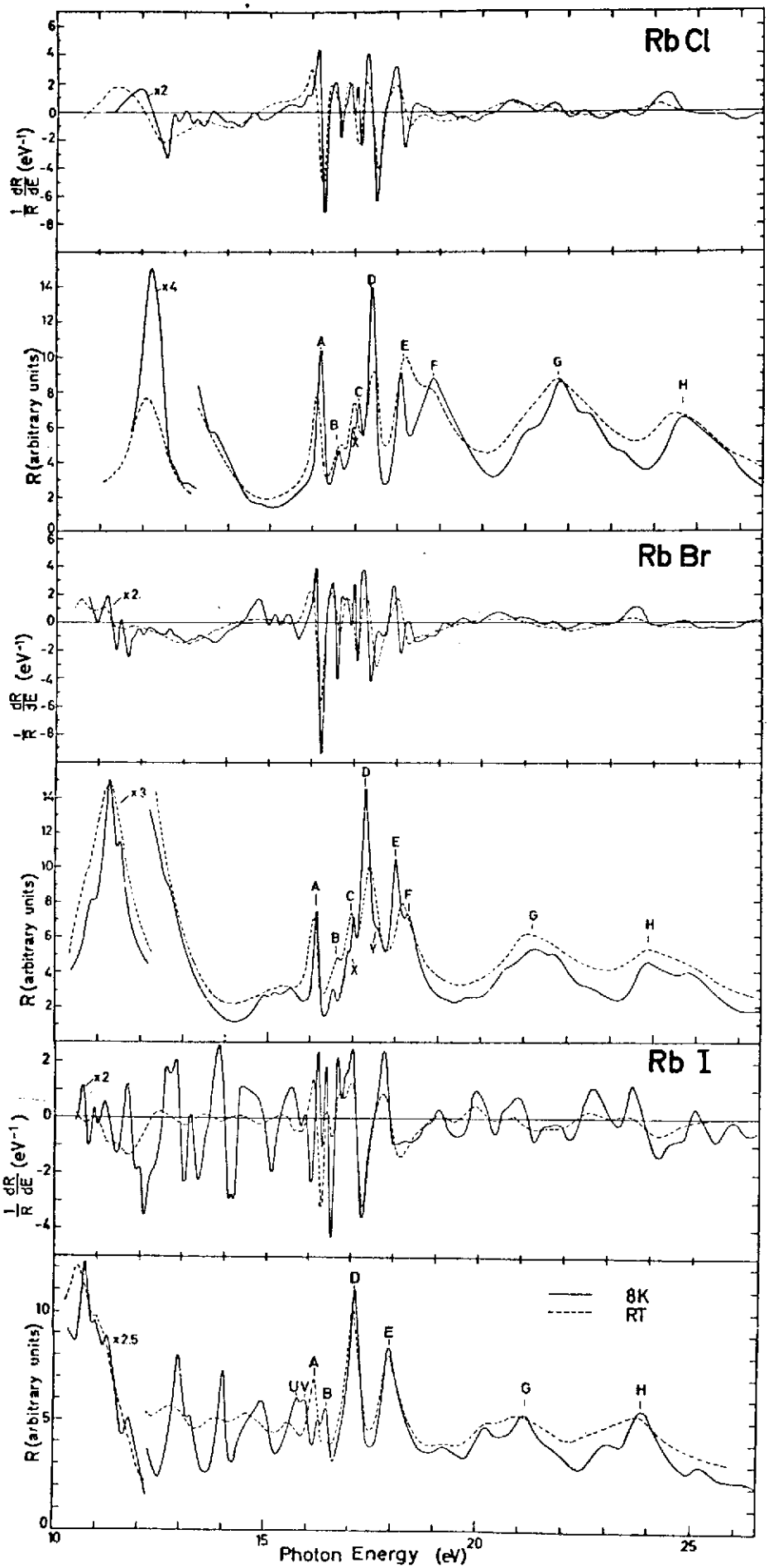
Rb Cl
Rb Br
Rb I
x2
x4
x3
x2.5
A
B
C
D
E
F
G
H
UV
X
8K
RT
R (arbitrary units)
Photon Energy (eV)

Fig. 2

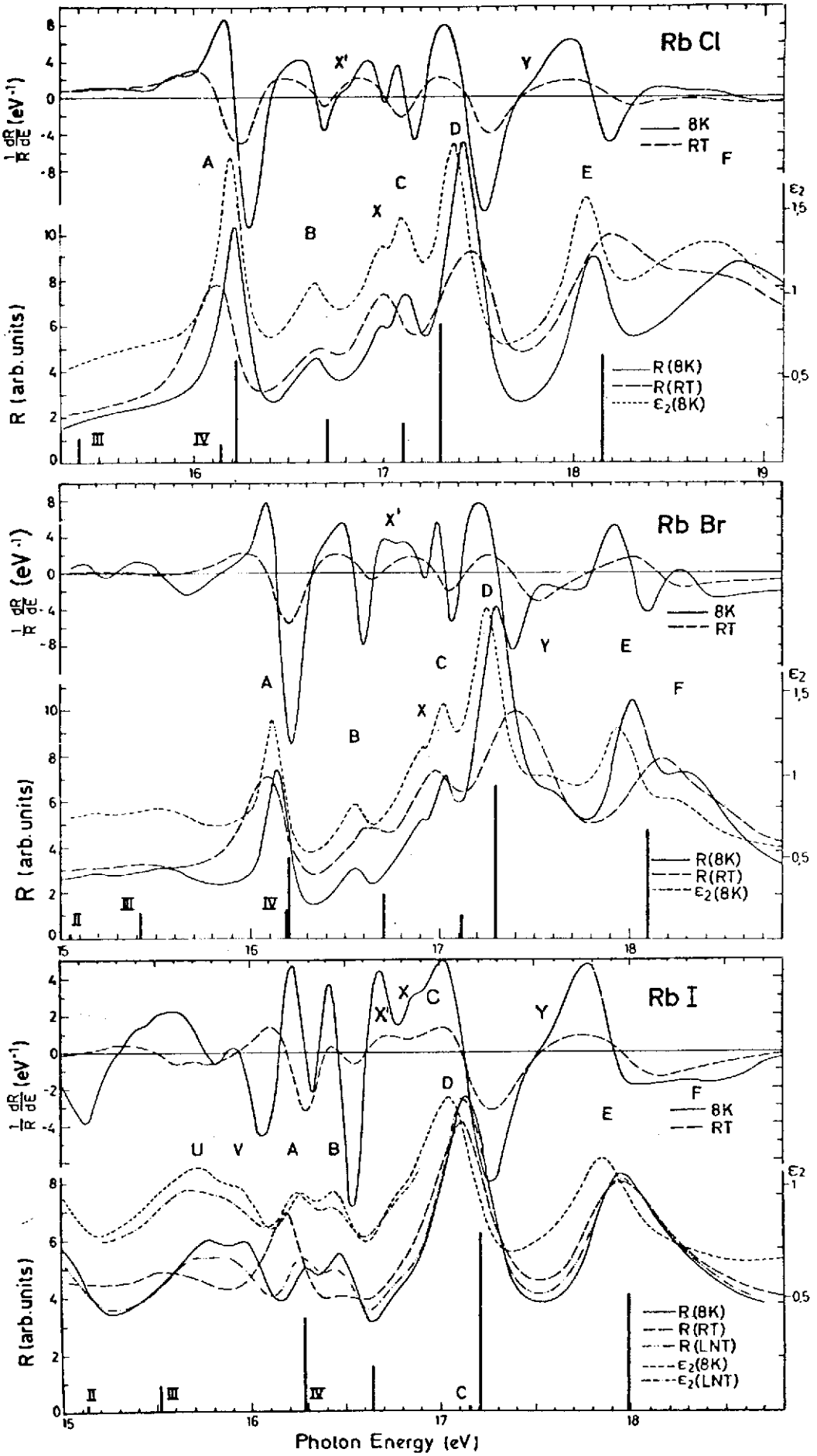
Rb Cl
Rb Br
Rb I
8K
RT
R(8K)
R(RT)
R(LNT)
ε2(8K)
ε2(LNT)
R (arb.units)
Photon Energy (eV)

Fig. 3

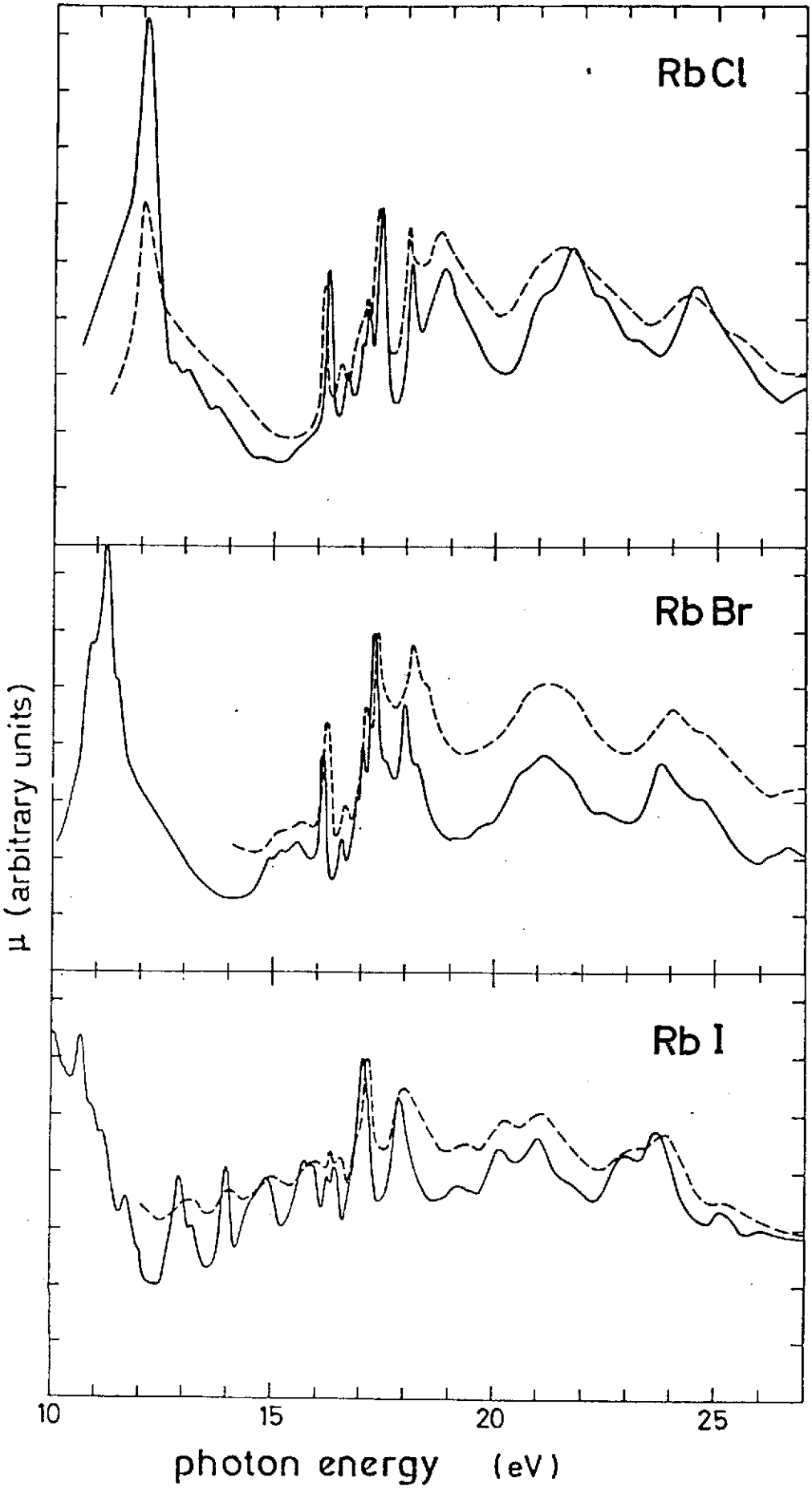

Fig. 4

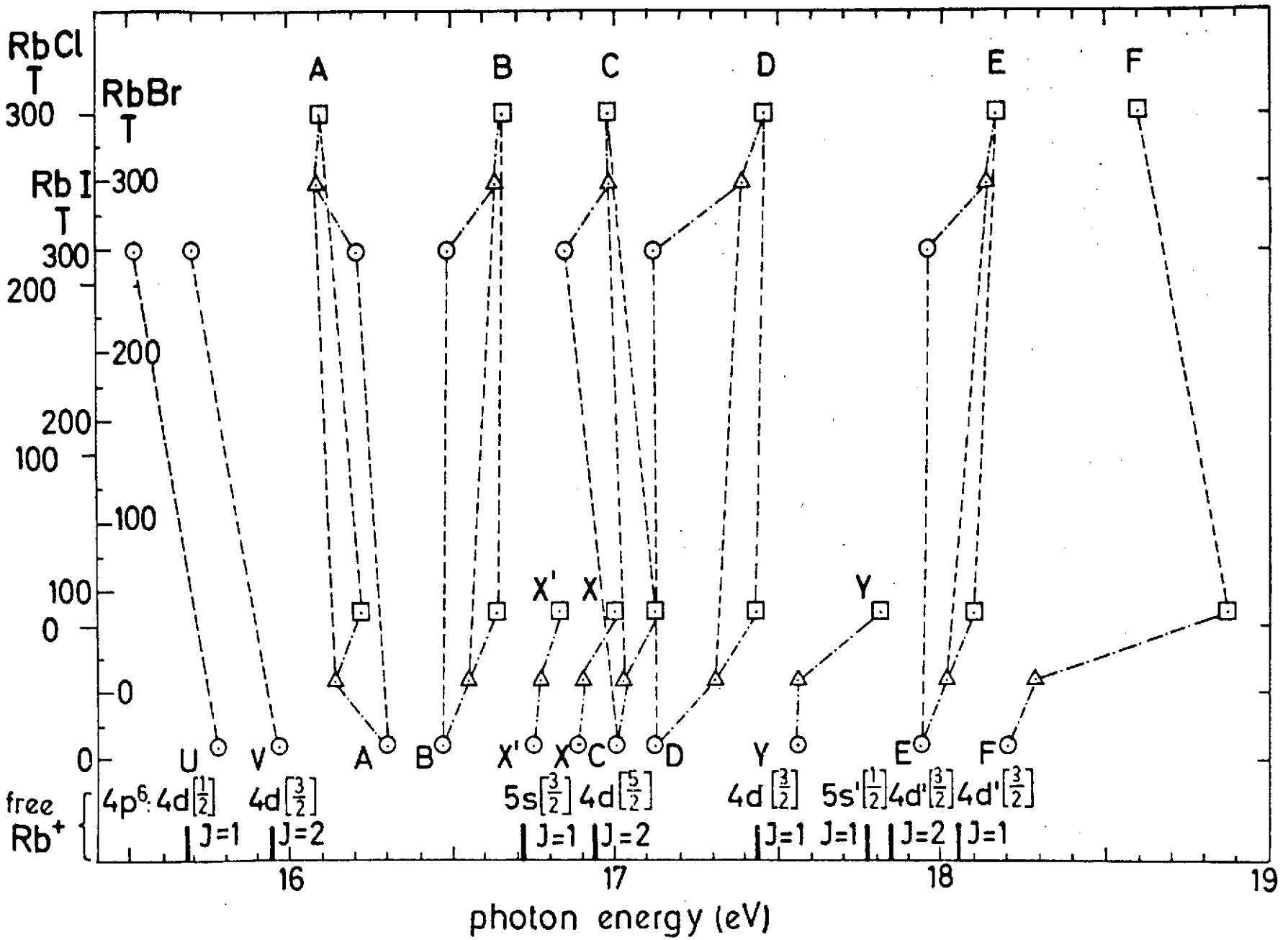
RbCl T
RbBr T
RbI T
300
300
300
200
200
200
100
100
100
0
0
0
A
B
C
D
E
F
X'
X'
Y
U
V
A
B
X'
X
C
D
Y
E
F
free Rb+
4p6 4d[1/2]
4d[3/2]
5s[3/2] 4d[5/2]
4d[3/2]
5s'[1/2] 4d'[3/2] 4d'[3/2]
J=1
J=2
J=1
J=2
J=1
J=1
J=2
J=1
16
17
18
19
photon energy (eV)

Fig. 5

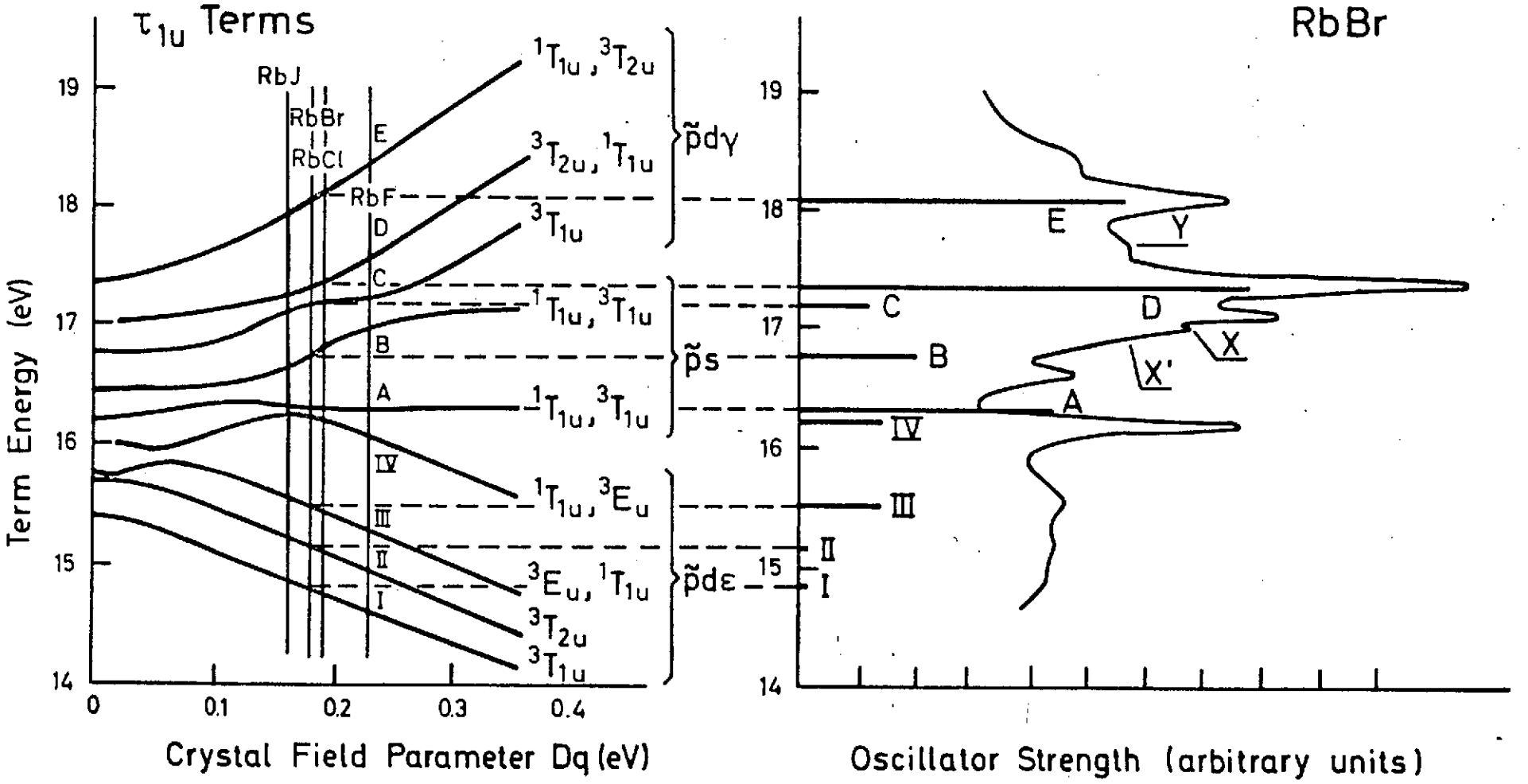
τ1u Terms
RbJ
RbBr
RbCl
RbF
E
D
C
B
A
IV
III
II
I
1T1u, 3T2u
3T2u, 1T1u
3T1u
1T1u, 3T1u
1T1u, 3T1u
1T1u, 3Eu
3Eu, 1T1u
3T2u
3T1u
p̃dγ
p̃s
p̃dε
Term Energy (eV)
19
18
17
16
15
14
0
0.1
0.2
0.3
0.4
Crystal Field Parameter Dq (eV)
RbBr
E
γ
C
D
X
X'
B
A
IV
III
II
I
Oscillator Strength (arbitrary units)

Fig. 6

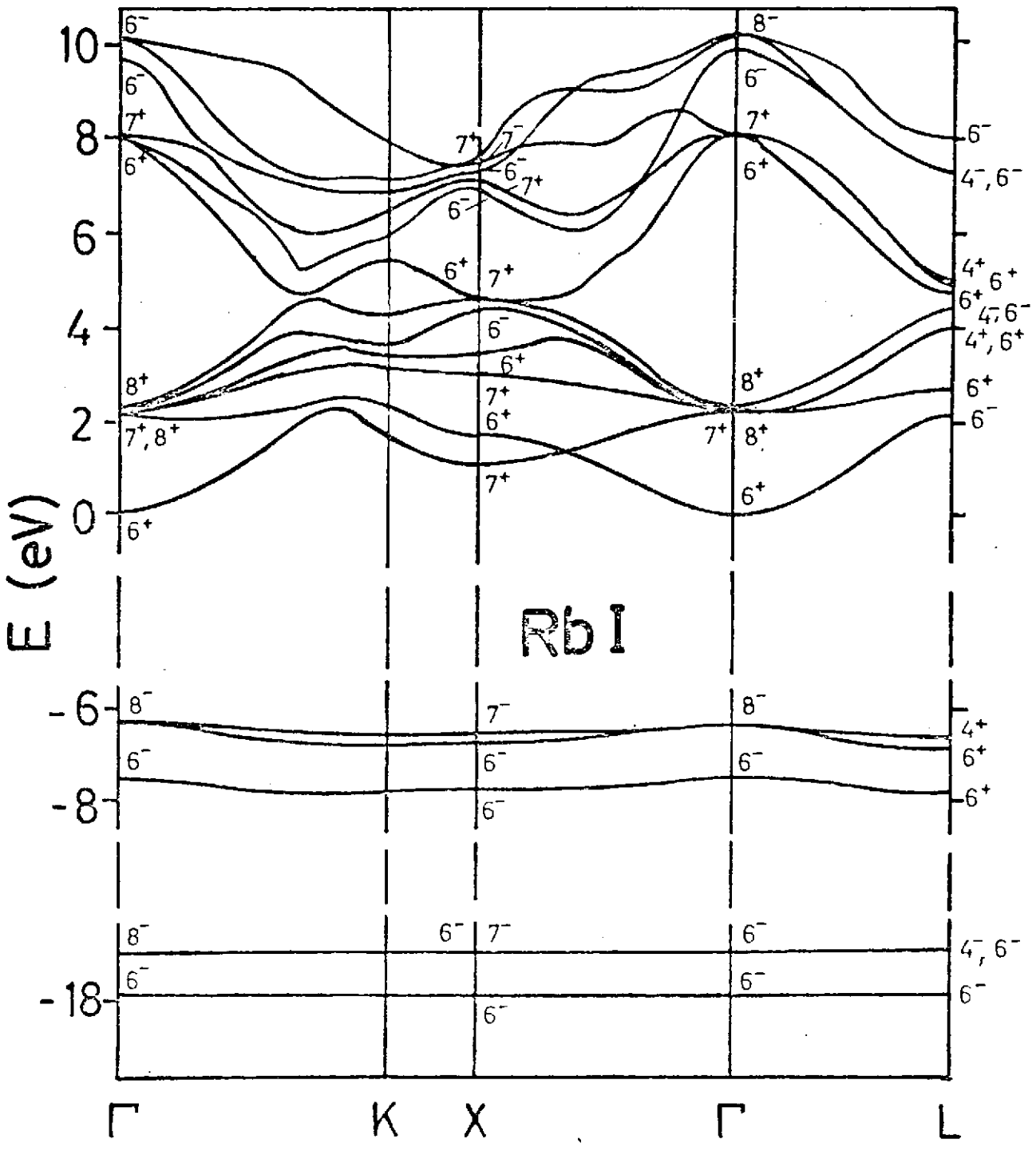

Fig. 7

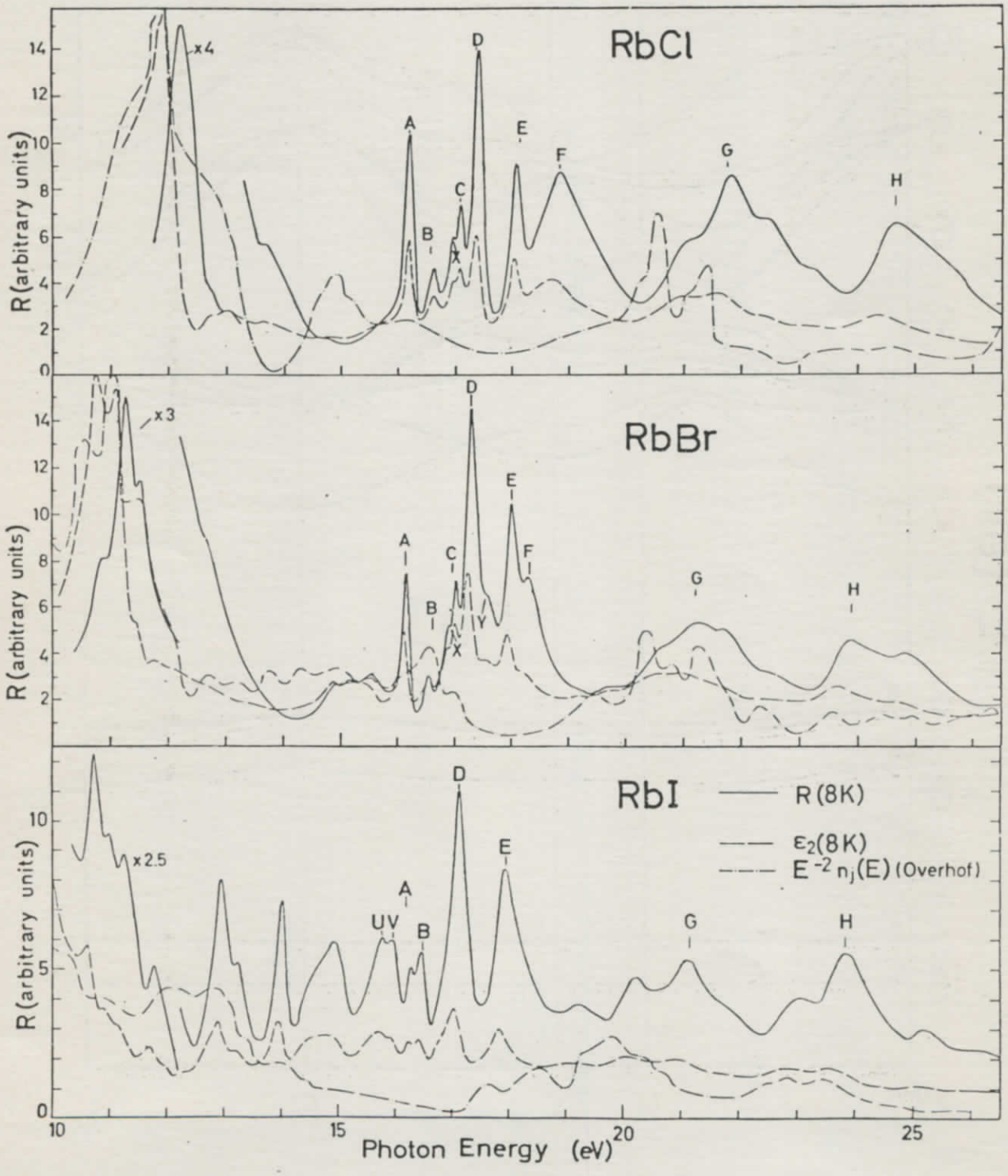
RbCl
RbBr
RbI
R (arbitrary units)
x4
x3
x2.5
A
B
C
D
E
F
G
H
X
Y
UV
R (8K)
ε2(8K)
E-2 nj(E) (Overhof)
Photon Energy (eV)
10
15
20
25

Fig. 8